

Finch: Fuzzing with Quantitative and Adaptive Hot-Bytes Identification

Tai D. Nguyen, Long H. Pham, Jun Sun

Abstract—Fuzzing has emerged as a powerful technique for finding security bugs in complicated real-world applications. American fuzzy lop (AFL), a leading fuzzing tool, has demonstrated its powerful bug finding ability through a vast number of reported CVEs. However, its random mutation strategy is unable to generate test inputs that satisfy complicated branching conditions (e.g., magic-byte comparisons, checksum tests, and nested if-statements), which are commonly used in image decoders/encoders, XML parsers, and checksum tools. Existing approaches (such as Steelix and Neuzz) on addressing this problem assume unrealistic assumptions such as we can satisfy the branch condition byte-to-byte or we can identify and focus on the important bytes in the input (called hot-bytes) once and for all. In this work, we propose an approach called Finch which is designed based on the following principles. First, there is a complicated relation between inputs and branching conditions and thus we need not only an expressive model to capture such relationship but also an informative measure so that we can learn such relationship effectively. Second, different branching conditions demand different hot-bytes and we must adjust our fuzzing strategy adaptively depending on which branches are the current bottleneck. We implement our approach as an open source project and compare its efficiency with other state-of-the-art fuzzers. Our evaluation results on 10 real-world programs and LAVA-M dataset show that Finch achieves sustained increases in branch coverage and discovers more bugs than other fuzzers.

Index Terms—Fuzzing, Hot-bytes, Neural Network

1 INTRODUCTION

Fuzzing has emerged as a powerful technique for finding security bugs in complicated real-world applications. It is used to find many reported CVEs in all sort of projects from compilers (e.g., gcc and clang), network tools (e.g., tcpdump and openssh), GNU softwares (e.g., readelf and objdump) to image processing libraries (e.g., libtiff and libpng). While the vast majority of the discovered bugs cause denial of service to commonly used software, some severe bugs such as remote code execution and privilege escalation are also detected.

In general, there are many types of fuzzing, e.g., white-box fuzzing, blackbox fuzzing, and greybox fuzzing. Among them, coverage-guided greybox fuzzing (CGF) is the most successful one. Its goal is to find test inputs that maximize code coverage within a given amount of time. Among many developed CGF tools, american fuzzy lop (AFL) is a leading fuzzer. It employs genetic algorithms to mutate user-provided test inputs and execute them to discover buggy behaviours. However, CGF fuzzers heavily rely on random mutations. This often prevents them from bypassing complicated branching conditions and thus leaves many vulnerabilities unreachable.

Common problems in fuzzing. Complicated branching conditions (e.g., magic-byte comparisons, checksum tests, and nested if-statements) are common obstacles that prevent CGF fuzzers from exploring more branches. An example of such conditions is shown in Figure 1 where bug #1 is protected by a checksum and bug #2 is covered if the first 4 bytes of the provided input equal to a magic number 0x6f56df77. It is obvious that covering these branches is non-trivial for CGF fuzzers as the probability of generating

```
1 u8 input[8];
2 // checksum test using nested if-statements
3 if (sum(input) < 8)
4     if (input[sum(input)] == 0x01)
5         bug(1);
6 // magic-byte comparison
7 if (u32(input) * 2 == 0xdeadbeef)
8     bug(2);
```

Fig. 1: Magic-byte comparisons and checksum tests

an exact combination of 4 bytes is negligible. To overcome such problems, different techniques have been proposed [1]–[7]. For instance, taint tracking and symbolic execution models have been applied to track the flow of input to the branching conditions. By doing that, hot-bytes are identified and then mutated more often than other bytes.

To detect hot-bytes but avoid unacceptable overhead of dynamic taint tracking or symbolic execution, existing approaches often propose their own lightweight taint algorithms. Notably, Angora [5] and GREYONE [4] record byte offsets which flow into each unsolved branching condition. REEDQUEEN [8] identifies input segments that are directly used in branching conditions. However, the lightweight taint algorithms are not able to capture the relation between inputs and branching conditions quantitatively (e.g., only byte offsets are returned). As a result, no clue on how to mutate hot-bytes is given. With the capability of capturing complicated dependency, deep neural networks have been recently considered as a complementary choice to tainting analysis. Neuzz [9] detects hot-bytes using a trained neural network. However, its approach is not adaptive as the guidance (i.e., gradient) quickly becomes outdated after several

branches are covered.

Our approach. In this paper, we propose a different fuzzing scheme. Let us assume that we are trying to bypass the true branch of $u32(input) * 2 == 0xdeadbeef$ given an initial test input t . A traditional fuzzer will repeatedly mutate t until one of its permutation t' satisfies the branch. Furthermore, even if hot bytes (the first four bytes) are identified, existing approaches have to exhaustively try every possible value in the worst case to cover the branch. In contrast, we use an expressive model (a neural network) to identify the hot-bytes and furthermore, we measure how far a test t is from covering the branch with a distance. In detail, we also mutate t , but t is replaced with t' if $|u32(t') * 2 - 0xdeadbeef| < |u32(t) * 2 - 0xdeadbeef|$. The comparison means that t' is better than t . With this approach, we gradually narrow down the difference between $u32(input) * 2$ and $0xdeadbeef$, and eventually bypass the targeted branch.

In general, we aim to systematically answer the following questions and design the fuzzer accordingly:

- Q1: How to quantitatively compare t and t' in term of which one is more likely to cover a branch? Inspired by search-based software testing [10]–[13], we propose a branch distance $f_n(t)$, which measure how far a branch br_n from being covered by a test input t . If $f_n(t') < f_n(t)$ then t' is better than t . In the above example, $f_n(t) = |u32(t) * 2 - 0xdeadbeef|$
- Q2: How to adaptively minimize fuzzing queue to reduce the number of redundant mutations? Existing approaches either use simple heuristics like keeping those tests which just cover some new branches as seeds (without considering whether covering those branches is meaningful for covering other uncovered branches), or keep mutating the same hot-bytes [9]. Such approaches are unlikely effective as during fuzzing, the branches to be covered keeps changing and thus the relevant seeds and the mutation strategy must be adaptive as well. To overcome the weakness above, we propose the min-Pareto set which is a lightweight fuzzing queue. If br_n is one of the targeted branches and $f_n(t')$ is minimal then t' belongs to the min-Pareto set.

We combine the answers of Q1 and Q2 in Finch, a smart adaptive fuzzer. We compare Finch with 6 state-of-the-art fuzzers including AFL [14], FairFuzz [15], Neuzz [9], MOPT [16], Angora [5], and TortoiseFuzz [17]. We conduct multiple experiments on LAVA-M and a set of test subjects including the latest versions of 10 high-profile real-world applications covering 7 different file formats, i.e., *jpg*, *png*, *xml*, *bz2*, *png*, *tiff*, and *ttf*. The experiment results show that Finch on average covers more branches and discovers many more unique crashes than all other fuzzers.

In summary, we make the following technical contributions:

- Our first contribution is an algorithm for fuzzing queue minimization which eliminates redundant mutations.
- Our second contribution is a novel machine learning approach for identifying hot-bytes, quantitatively and adaptively.

- Our third contribution is an open-source fuzzer, named Finch, which is systematically evaluated on extensive experiments.

The remainder of the paper is organized as follows. Section 2 provides relevant background on fuzzing, with a review of key innovations of AFL. Section 3 presents our fuzzing approach. Section 4 shows implementation details. Section 5 reports evaluation results. Section 6 reviews related work and Section 7 concludes the paper.

2 PRELIMINARY

In this section, we define the fuzzing problem and review existing most relevant grey-box fuzzing approaches.

2.1 Problem definition

Let P be the program under test; and B be the set of basic blocks (i.e., non-branching block of codes) in P . Formally, a program can be represented as a *control flow graph*, in which each node represents a basic block and each edge (a.k.a branch) represents a transition between 2 blocks. Ideally, as a testing engine, a fuzzer’s goal is to generate a test set which can expose all bugs in the program. However, since we do not know where the bugs are, normally a fuzzer aims to generate a test set with high code coverage. This is based on the observation that *increasing code coverage often results in more bugs found* [15]. Among different types of code coverage (e.g., block coverage and path coverage), edge coverage is the most popular choice, as it balances between effectiveness and efficiency.

In this work, we define a branch e in the program as a pair of blocks (x, y) with $x, y \in B$. Let E is the set which contains all possible branches of the program P . A test input t is said to cover the branch $e = (x, y)$ iff its execution has a transition from x to y . We define a set of branches that are covered by a test input t as E_t . Our problem is then defined formally as follows. *Given a program P and a set of seed tests T_0 , generate a new set of test inputs T which maximizes the number of covered branches $|C|$ in the program, where $C = \cup_{t \in T} (E_t)$, and do so as early as possible.*

2.2 AFL overview

Among multiple developed fuzzers, AFL is an industrial standard one that employs genetic algorithms to maximum code coverage. Many fuzzers are built on top of or inspired by AFL. In the following, we briefly introduce AFL by explaining its key components.

Fuzzing procedure. The main workflow of AFL is shown in Algorithm 1. The inputs of the procedure are the program under test P , the set of original user-provided test inputs T_0 , and the expected fuzzing time. In general, AFL generates new test inputs by mutating a set of existing ones, called *seed pool*. Initially, the seed pool contains only the user-provided test inputs (line 1). During each iteration, AFL picks a random test input from the seed pool (line 5), mutates it to generate new test inputs (line 6), and runs the mutated inputs with the target program (line 7). The

Algorithm 1: $fuzz(P, T_0, time)$

```

1 let seed_pool  $\leftarrow T_0$ ;
2 let crash_pool  $\leftarrow \emptyset$ ;
3 while in time limit do
4   let new_seeds  $\leftarrow \emptyset$ ;
5   foreach t in seed_pool do
6     foreach t' in mutate(t) do
7       let r  $\leftarrow execute(t')$ ;
8       if r causes buggy behaviours then
9         crash_pool.add(t');
10      else if r obtains new coverage then
11        new_seeds.add(t');
12   seed_pool  $\leftarrow seed\_pool \cup new\_seeds$ ;
13 return seed_pool, crash_pool;

```

execution is monitored by the fuzzer to collect necessary information. If the test input execution causes some buggy behaviours (e.g., makes the program crash or hang), the test input is added into a *crash pool* and is used to debug the program later (lines 8-9). If the test input executes some new branches in the program, it is added into the seed pool and will be mutated to generate more test inputs in the next iteration (lines 10-11). In case the test input does not cause any buggy behaviours nor cover any new branch, it is deemed irrelevant and simply discarded. The process continues until the time budget is exhausted. At that time, all the test inputs in the seed pool and the crash pool are returned. The output of the procedure is a set of test inputs, each of which covers some unique branches in the program or causes some buggy behaviours.

Mutation stages. A test input is a sequence of bytes. In AFL, each test input is mutated in two stages: *deterministic* stage and *havoc* stage. Mutations are based on a set of different byte-level mutation operators. Currently, there are 11 mutation operators [16] in AFL. In the deterministic stage, the mutation operators are applied deterministically based on a predefined algorithm. For instance, given a test input, the *bit_flip* operator is applied before the *byte_flip* operator. Therefore, the mutation results are identical given the same input in the deterministic stage. Due to this reason, deterministic mutations only need to be applied once for the same test input. So a test input is passed through the deterministic stage iff it has not been mutated previously. In contrast, the havoc stage randomly applies mutation operators on the test inputs. Thus given the same input, it can generate different new mutants and can be invoked multiple times. Additionally, the havoc stage often changes the size of a test input by adding or deleting multiple block of bytes.

As mutation strategies have a huge impact on AFL's effectiveness, extensive studies have been conducted on improving AFL's mutation strategy. It can be improved in multiple ways, e.g., using dictionary collected from static analysis [1], using symbolic execution to solve constraints [5], and analyzing data/control dependency at run-time [4]. However, the more intelligent the improvement is, the more

run-time information needed and thus the more overhead introduced into the fuzzer. Therefore, how to design a mutation strategy which is both effective and efficient is still an ongoing research problem.

Edge coverage. From Algorithm 1, it can be noted that discovering test inputs with new coverage is essential for AFL's performance. When no new branches are covered, AFL becomes more or less a simple random test input generation engine. To collect the coverage information, AFL injects a small piece of code that captures the control flow of the target program. The injected code associate each basic block with a random numeral identifier. The identifier of the branch (x, y) is then computed from the identifiers of blocks x and y as follows:

$$ID_{(x,y)} = (ID_x \gg 1) \oplus ID_y$$

where \gg and \oplus are right-shift and xor operators respectively. AFL keeps track of coverage branches in a bitmap and uses the above formula to compute the key value for a branch access. Initially, the values of all the keys are unset. Then in the execution of each test input, AFL monitors the transitions between the basic blocks in the program. Whenever there is a transition from a block x to another block y , the according branch identifier $ID_{(x,y)}$ is computed. In case the value at the key $ID_{(x,y)}$ is unset, it is now set and the test input is deemed to cover a new branch (x, y) .

3 OUR APPROACH

To bypass complicated branching conditions, we build a fuzzing tool named Finch. The novelty of Finch is twofold. First, Finch identifies hot-bytes with an expressive neural network model. Second, Finch measures the effectiveness of mutations on the hot-bytes quantitatively by maintaining a lightweight seed pool, called *min-Pareto set*. The min-Pareto set is adaptive as it contains the seeds which have one-to-one correspondence to the branches to be covered next. This strategy helps us focus more on the test inputs which have potential to uncover new branches. Moreover, in our neural network model, test inputs chosen from the min-Pareto set are labeled with the distances measures, instead of coarse-grained coverage information. We will give the details about branch distance, how we choose the test inputs to mutate, how we train the model and use it to predict hot-bytes in subsequent sections.

3.1 Branch distance

Inspired by search-based software testing [10]–[13], we compute the distance between each test input and uncovered branches in the program. The distance often contains two components: approach distance and branch distance. Intuitively, the approach distance and branch distance measure the gap between two execution paths and two branches of a node respectively. As the concrete control flow graph of a target program is explored on the fly, it is expensive to maintain approach distance [13] and thus, we focus on

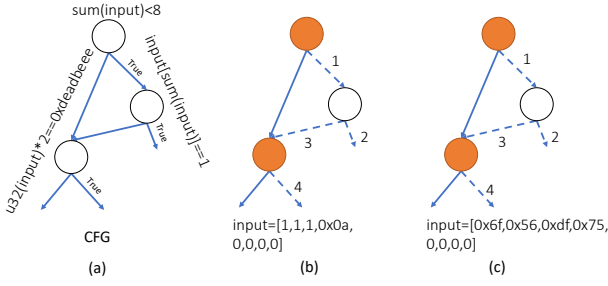


Fig. 2: An example to demonstrate how a branch distance bitmap is computed

the branch distance (so as to avoid overwhelming computational overhead). In the following, we define our customized branch distance.

Let $f_n(t)$ be a function to measure how far the test input t is from covering an uncovered branch br_n . Let us assume that br_n is an outgoing uncovered branch from a branching node n and n is labeled with a condition c . At the byte-code level, c is one of the following forms $true$, $false$, $a > b$, $a \geq b$, $a \leq b$, $a < b$, $a = b$, $a \neq b$ where a and b are either a constant or a variable. The function $f_n(t)$ is then computed as follows

$$f_n(t) = \begin{cases} |a - b| & \text{if } t \text{ visits node } n \\ K & \text{otherwise} \end{cases}$$

where K is a constant representing the maximum distance. If c is either $true$ or $false$ then $|a - b|$ is 0. The function $f_n(t)$ is defined such that the closer the branch is from being covered, the smaller the resultant value is.

For a program with n uncovered branches, we define the branch distance bitmap of a test input t as follows.

$$f(t) = \{f_1(t), f_2(t), \dots, f_n(t)\}$$

Example 1. Fig. 2(a) shows the control flow graph of the program shown in Fig. 1. Suppose we execute the program with 2 different test inputs, t_0 with $input=[1,1,1,0x0a,0,0,0,0]$ and t_1 with $input=[0x6f,0x56,0xdf,0x75,0,0,0,0]$. The execution paths of t_0 and t_1 are shown in Fig. 2(b) and 2(c), where visited nodes are highlighted in orange; dashed and solid lines indicate uncovered and covered branches respectively. With these 2 test inputs, there are 4 uncovered branches left in the program, which are marked with the number 1, 2, 3, and 4. Applying the above formula, we have $f_1(t_0) = |13 - 8| = 5$ and $f_4(t_0) = |0x0101010a * 2 - 0xdeadbeef| = 3702242522$. The value of $f_2(t_0)$ and $f_3(t_0)$ are K because t_0 does not visit the node with branch 2 and 3 as its outgoing branches.

So the branch distance bitmap of t_0 is:

$$\begin{aligned} f(t_0) &= \{f_1(t_0), f_2(t_0), f_3(t_0), f_4(t_0)\} \\ &= \{5, K, K, 3702242522\} \end{aligned}$$

Similarly, the branch distance bitmap of t_1 is:

$$f(t_1) = \{f_1(t_1), f_2(t_1), f_3(t_1), f_4(t_1)\} = \{529, K, K, 4\}$$

3.2 Choosing test inputs

We interpret the problem of fuzzing a program as a multi-objectives optimization problem, which can be formulated as

$$\min_{t \in T} (f_1(t), f_2(t), \dots, f_n(t))$$

where $f_n(t)$ returns the quantitative distance between a test input t and an uncovered branch br_n ; T is a set of all possible test inputs. In general, there does not typically exist a test input t that minimizes all distances simultaneously. So instead, we accept a test input t as a solution as long as it is Pareto optimal, which is determined by a dominance.

In detail, a feasible solution t_1 is said to dominate another solution t_2 iff

- (1) For all objectives, t_1 is not worse than t_2 . Formally, $\forall i \in \{1, 2, \dots, n\} \cdot f_i(t_1) \leq f_i(t_2)$.
- (2) There exists an objective that t_1 is strictly better than t_2 . Formally, $\exists j \in \{1, 2, \dots, n\} \cdot f_j(t_1) < f_j(t_2)$.

With the above definition, a solution t is a Pareto optimal solution if there does not exist another solution that dominates it. A set of Pareto optimal solutions lie on a Pareto boundary.

A naive strategy is to simply select the test inputs which satisfy the Pareto optimal conditions to mutate in each generation. However, a known problem [10] for such a strategy is that the number of Pareto optimal test inputs soars after a few generations. To overcome the problem, we apply 2 rules to reduce the number of test inputs in the Pareto boundary. The remaining test inputs after filtering are called min-Pareto set and are used to mutate.

The rules are designed as follows:

- (r1) Removing 'future' objectives: let br_k be an outgoing uncovered branch of a node k in a control flow graph, an objective f_k is removed from our list of objectives if the node k is never visited. Intuitively, because node k is never visited, covering br_k is not an immediate objective yet (rather covering some branches leading to node k is). Furthermore, since node k is never visited, we are not able to compute the distance measure and the model is unlikely able to predict meaningfully either. We call the branches according to the remaining objectives after filtering *just-missed branches*.
- (r2) Removing 'redundant' test inputs: a Pareto optimal test input t is removed from a set of Pareto optimal test inputs O if $\forall i \in \{1, 2, \dots, n\}; \exists t' \in O; t' \neq t; f_i(t') \leq f_i(t)$. Intuitively, we remove a test input t if for all objectives, there always exists some other test inputs which are better than t . We notice that the Pareto boundary is not changed this way.

Ideally, we want to find a set with a minimum number of test inputs which satisfy the above 2 rules. However, due to the complexity of rule r2, instead of finding the optimal set of test inputs, we use a greedy algorithm that approximates a min-Pareto set S from the original Pareto set O in order to reduce computational resources. The overall workflow is shown in Algorithm 2. Let J_t be the set of objectives f_n such that $\forall t' \in T; t' \neq t; f_n(t) \leq f_n(t')$. The main idea of our algorithm is to sort test inputs $t \in O$

Algorithm 2: $\text{min_pareto_set}(O)$

```

1 let  $S \leftarrow \emptyset$ ;
2 let  $\text{sorted\_list} \leftarrow \text{descending\_sort}(O)$ ;
3 while  $\text{sorted\_list} \neq \emptyset$  do
4    $(t, J_t) \leftarrow \text{sorted\_list.pop\_front}()$ ;
5   if  $J_t \neq \emptyset$  then
6      $S.add(t)$ ;
7     foreach  $(t', J_{t'})$  in  $\text{sorted\_list}$  do
8        $J_{t'} \leftarrow J_{t'} \setminus J_t$ ;
9 return  $S$ ;

```

in a descending order of $|J_t|$ (line 2) and then check the test input one by one according to the sorted list (lines 3-4). For each t , if $J_t \neq \emptyset$ then t is added to S (lines 5-6). After that, for all remaining test inputs t' in the list, we update $J_{t'} = J_{t'} \setminus J_t$ (lines 7-8) before checking the next element in the next iteration. Since O is sorted only once, our algorithm only returns an approximated result for the min-Pareto set with complexity $|O|^2$.

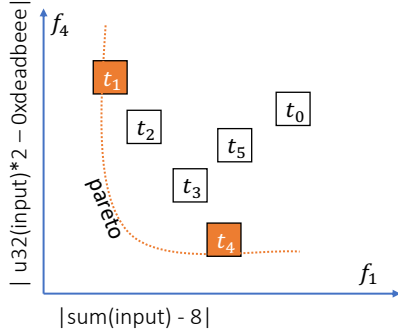


Fig. 3: Two objectives optimization for the code in Fig. 1

Example 2. Fig. 3 illustrates the simplified multiple-objectives problem from Fig. 1, in which we only consider 2 conditions at line 3 and 7. The x-axis and the y-axis represent objective functions f_1 and f_4 respectively. According to the returned values of f_1 and f_4 , a test input t occupies a position $(f_1(t), f_4(t))$ on xy -plane. Suppose t_0 is the original test inputs and the mutation creates test inputs from t_1 to t_5 . In case the new test inputs do not cover new branches, other fuzzers (e.g., AFL and Angora) simply discards all of them and starts a new mutation process with t_0 again. Our approach, on the other hand, computes the distances between the new test inputs and the uncovered branches. We then detect that t_1 and t_4 , although not cover new branches, are on the Pareto boundary and are better solutions than t_0 . So instead of discarding all generated test inputs, we update the seed pool by adding Pareto optimal test inputs t_1, t_4 . After running Algorithm 2, while t_0 is removed from the seed pool, t_1 and t_4 are kept and ready to be mutated to generate new test inputs. So although no new coverage is obtained, the seed pool makes some steps toward uncovered branches. The strategy is repeated until both branches are covered.

3.3 Hot-bytes prediction

For each generation, the test inputs in the min-Pareto set are used for mutation. However, unlike AFL, where all bytes of the test inputs are mutated equally, we only focus on mutating hot-bytes of each test input. Intuitively, hot-bytes should be selected such that mutating them is more likely to cover new branches (than mutating other bytes).

Our idea is to predict the hot-bytes using a neural network model. The novelty of our approach is the training data and the labels. First, instead of using all generated test inputs, we only use the test inputs in the min-Pareto set, which is chosen based on Algorithm 2. This approach helps to reduce the overhead in the training process, while still keeping most informative and updated training data. Second, instead of using the coarse-grained coverage information as the label, our model is trained with the branch distance bitmaps of the test inputs. With the training data, our model can predict which bytes need to be mutated to decrease the values of the distances between test inputs and uncovered branches.

The number of neurons at the input layer is equal to the number of bytes of the longest test input in the training data. The number of neurons at the output layer is equal to the number of just-missed branches in the program. The test inputs are normalized by padding zero to guarantee all the test inputs have the same length as the longest one. The branch distance bitmap is also normalized by dividing by K so that the branch distance bitmap has values ranging from 0 to 1.

In the training process, we use binary cross-entropy to compute the loss between a predicted branch distance bitmap \hat{y} and the ground truth $y = f(t)/K$. It is defined as follows.

$$\text{loss}(y, \hat{y}) = -\frac{1}{n} \sum_{i=0}^n (y_i \times \log(\hat{y}_i) + (1 - y_i) \times \log(1 - \hat{y}_i))$$

Note that $y_i = 1$ represents the maximum branch distance, which is incomparable with other values by nature. Therefore, we simply set $\hat{y}_i = y_i$ if $y_i = 1$ to discard the loss between y_i and \hat{y}_i .

After having the model, we can use it to predict hot-bytes of the test inputs. In particular, each test input in the min-Pareto set is fed into the model. After training, we can compute the gradients of each byte in the test input according to the model prediction.

Example 3. Suppose that we want to mutate a test input t with $\text{input}=[1,1,1,0x0a,0,0,0,0]$. Our trained model receives t and outputs gradient scores $g=[0.5,0.5,0.5,0.9,0,0,0,0]$. The magnitude of g means that the first 4 bytes are more important than others. The sign of g means that we should decrease the values of the first 4 bytes to cover new branches.

3.4 Hot-bytes mutation

Given a test input t , in this section, we will explain how t 's hot-bytes are mutated. The mutation algorithm is firstly introduced by [9]. It is summarized in Algorithm 3. Since it is impossible to exhaustively mutate all bytes in t , the key idea is that we consider a group of bytes as a single byte

Algorithm 3: *mutate_hot_bytes(t, model)*

```

1 let  $T \leftarrow \emptyset$ ;
2 let  $g \leftarrow \text{model}(t)$ ;
3 foreach  $\text{range}$  in  $[(0, 2), (2, 4), (4, 8), \dots]$  do
4   let  $\text{locs} \leftarrow \text{top}(g, \text{range})$ ;
5   foreach  $\text{dir}$  in  $[-1, 1]$  do
6      $t' \leftarrow t.\text{copy}()$ ;
7     while  $\exists x \in t'[\text{locs}]; x \neq 0 \wedge x \neq 255$  do
8        $t'[\text{locs}] \leftarrow t'[\text{locs}] + \text{dir} * \text{signs}(g[\text{locs}])$ ;
9        $T.\text{add}(t')$ ;
10 return  $T$ ;

```

and exhaustively mutate them. The more important bytes is grouped into a smaller group and less important bytes are grouped into a larger group (line 3-4). Each byte in a group is increased or decreased according to the sign of its gradient (line 8).

First, we compute the gradient scores g using the trained model (line 2). Then, each group of sorted bytes are repeatedly selected for mutation until all bytes are grouped (line 3-4). For each group of selected bytes, we gradually increase or decrease their values by 1 (line 8) until all of them reach their boundaries (line 7). Note that function $\text{sign}(x)$ returns 1 if $x > 0$, 0 if $x = 0$ and -1 if $x < 0$ and thus, $\text{signs}(g[\text{locs}])$ returns a list of $\text{sign}(x)$ where $x \in g[\text{locs}]$.

Example 4. Suppose that we want to mutate a test input t with $\text{input}=[1,1,1,0x0a,0,0,0,0]$. Our trained model receives t and outputs gradient scores $g=[0.5,0.5,0.5,0.9,0,0,0,0]$. According to algorithm 3, t is mutated as follows:

- Going up ($\text{dir}=1, \text{range}=(2,4)$): input is added to the corresponding signs. The possible permutations of input are: $[1,1,2,0x0b,0,0,0,0]$, $[1,1,3,0x0c,0,0,0,0]$, \dots , $[1,1,0xf6,0xff,0,0,0,0]$, \dots , $[1,1,0xff,0xff,0,0,0,0]$
- Going down ($\text{dir}=-1, \text{range}=(2,4)$): input is subtracted to the corresponding signs. The possible permutations of input are: $[1,1,0,0x09,0,0,0,0]$, $[1,1,0,0x08,0,0,0,0]$, \dots , $[1,1,0,0x06,0,0,0,0]$, \dots , $[1,1,0,0,0,0,0,0]$

3.5 System overview

We are now ready to present the overall workflow of Finch shown in Algorithm 4. The difference between Finch and AFL is highlighted in orange. Initially, we compute the min-Pareto set seed pool according to the original user-provided test inputs (line 1). While time is available during each iteration, we train a model according to the current test inputs in seed pool and their branch distance bitmaps (line 4). After having the model, in the mutation stage, we use Algorithm 3 to predict the hot-bytes and mutate each test input in the seed pool to get the new test inputs. Based on the execution of the new test inputs, they may be added into the crash pool (lines 10-11) or the new seeds (lines 12-13). Note that unlike AFL, the new test input does not need to cover any new branch to be added into *new_seeds*. After mutating all the test input in the current

Algorithm 4: *hot_fuzz(P, T_0 , time)*

```

1 let  $\text{seed\_pool} \leftarrow \text{min\_pareto\_set}(T_0)$ ;
2 let  $\text{crash\_pool} \leftarrow \emptyset$ ;
3 while in time limit do
4   let  $\text{model} \leftarrow \text{train\_model}(\text{seed\_pool})$ ;
5   let  $\text{new\_seeds} \leftarrow \emptyset$ ;
6   foreach  $t$  in  $\text{seed\_pool}$  do
7     let  $T \leftarrow \text{mutate\_hot\_bytes}(t, \text{model}) \cup \text{havoc}(t)$ ;
8     foreach  $t'$  in  $T$  do
9       let  $r \leftarrow \text{execute}(t')$ ;
10      if  $r$  causes buggy behaviours then
11         $\text{crash\_pool}.\text{add}(t')$ ;
12      else if  $r$  is on Pareto boundary then
13         $\text{new\_seeds}.\text{add}(t')$ ;
14    $\text{seed\_pool} \leftarrow \text{seed\_pool} \cup \text{new\_seeds}$ ;
15    $\text{seed\_pool} \leftarrow \text{min\_pareto\_set}(\text{seed\_pool})$ ;
16 return  $\text{seed\_pool}, \text{crash\_pool}$ ;

```

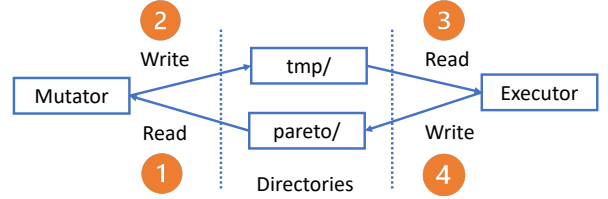


Fig. 4: The modular architecture of Finch

seed pool, all the test inputs in *new_seeds* are added into *seed_pool* (line 14) and then we apply the function to find the min-Pareto set in *seed_pool* again (line 15) before beginning the new iteration. Like AFL, the output of Finch is the set of test inputs in *seed_pool* and *crash_pool* (line 16).

4 IMPLEMENTATION

Finch is implemented in C and Python with an estimated 4k lines of code. It has two main components: *mutator* and *executor*. While Python is adopted to implement a *mutator* due to the ease of neural network implementation using PyTorch, we choose C to implement the *executor* to minimize the execution time and reuse some components of AFL. Fig. 4 presents the general workflow of Finch. The *mutator* evolves the Pareto optimal test inputs located at the directory *pareto/*. After that, it writes generated test inputs to the directory *tmp/* and asks the *mutator* to execute them. If an executed test input is Pareto optimal, the *executor* sends it back to the directory *pareto/*. Otherwise, it is deleted. The cycle continues until Finch reaches predefined time limit (e.g., 24h). Note that test inputs located at directory *pareto/* are Pareto optimal and they must go through the Algorithm 2 implemented in *mutator* to form a min-Pareto set. *Neural Network Architecture*. Our neural network is implemented in PyTorch version 1.6.0. It has one hidden fully-connected layer. The input and output layers use activation function ReLU and Sigmoid respectively. A neural network is trained for 200 epochs and deleted after assisting the gradient-guided mutation. Since our neural network is simple, the

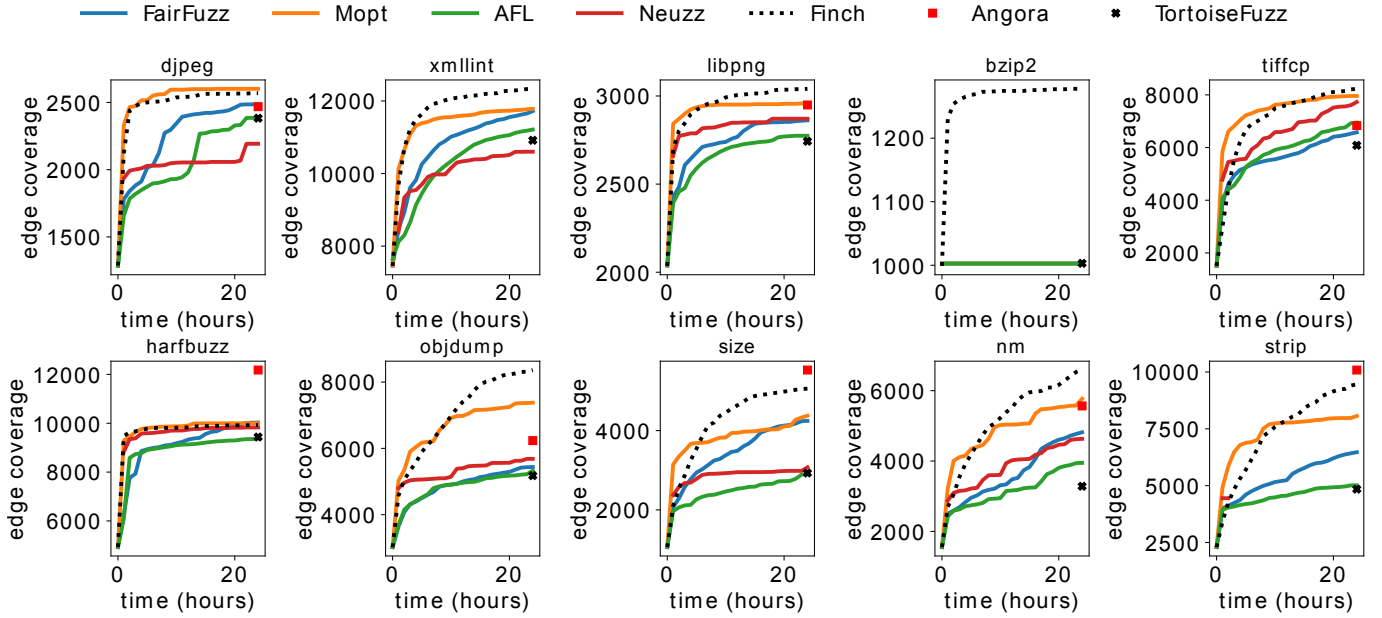


Fig. 5: Edge coverage of different fuzzers running for 24 hours

training time is often less than 1 minute. A feed-forward neural network is preferred to keep Finch efficient and relatively explainable.

Instrumentation. To construct a branch-distance bitmap from a test input, we write an LLVM Pass to inject our handlers, which capture operands of conditional instructions, i.e., *BranchInst* and *SwitchInst* at run-time. Due to many different data types used in a comparison, for any comparison that we are unable to derive branch distance, the default distance 0 is used. More specifically, we maintain another shared memory along with AFL’s coverage bitmap to save branch distances of both uncovered and covered branches. From these two bitmaps, we are able to infer which branch is uncovered and its corresponding distance. Note that to avoid instrument overhead, instead of making a function call to compute branch distance $|a - b|$ for every comparison instruction, we use single instruction *xor* to compute distance, i.e., $a \oplus b$. The xor distance guarantees that if a equals to b then branch distance is 0. Although the *xor* operator is used, our metric provides greater granularity (i.e., the returned value ranges from 0 to $2^n - 1$ where n is the number of bits representing data) compared to CMP feedback [18], [19] (i.e., the returned value ranges from 0 to n).

5 EVALUATION

In this section, we evaluate Finch through multiple experiments on two different types of datasets: 10 real-world applications and LAVA-M [1] benchmark with injected bugs. The experiments are designed to answer the following research questions (RQ).

- RQ1: Can Finch achieve higher edge coverage than existing fuzzers?
- RQ2: Is the branch-distance bitmap useful?
- RQ3: How min-Pareto set help increase edge coverage?

Package	Program
binutils-2.36	<code>objdump -D @@</code>
	<code>nm-new -C @@</code>
	<code>size @@</code>
	<code>strip-new @@ -o tmp_file</code>
libjpeg-turbo-2.0.6	<code>djpeg @@</code>
libpng-1.6.37	<code>libpng_read_fuzzer @@</code>
bzip2-1.0.8	<code>bzip2 -dk @@</code>
harfbuzz-2.8.0	<code>hb-draw-fuzzer @@</code>
libxml2-2.9.10	<code>xmllint @@</code>
tiff-4.2.0	<code>tiffcp -c lzma @@ tmp.tiff</code>

(a) Programs used in our experiments

Fuzzer	Technical details
AFL [14]	Evolutionary search
FairFuzz [15]	Evolutionary search + rare branches
Neuzz [9]	Evolutionary search + neural network
MOPT [16]	Evolutionary search + particle swarm
Angora [5]	Evolutionary search + taint tracking
TortoiseFuzz [17]	Evolutionary search + memory operation favor

(b) State-of-the-art fuzzers used in our experiments

TABLE 1: Experiment setup

- RQ4: Can Finch find more bugs than existing fuzzers?
- RQ5: What is the overhead of training model?

We compare Finch with 6 state-of-the-art fuzzers on the 10 real-world applications, as shown in Table 1. While MOPT and FairFuzz achieve relatively high edge coverage in many evaluations [20], [21], Angora and Neuzz focus on mutating hot-bytes, which is similar to Finch. TortoiseFuzz [17] has been published recently. The initial test inputs are collected from their repositories with the file size limit of 10 kb. All experimental results reported below are obtained on an Ubuntu Ubuntu 16.04 LTS machine with Intel Core(TM) i9 and 32GB of memory.

Program	Tortoise Fuzz	Angora	MOPT	FairFuzz	AFL	Neuzz	Finch
<i>djpeg</i>	2383	2469	2602	2486	2386	2193	2569
<i>xmllint</i>	10916	n/a	11779	11718	11211	10601	12329
<i>libpng</i>	2743	2949	2958	2862	2774	2871	3041
<i>bzip2</i>	999	n/a	999	999	999	n/a	1278
<i>tiffcp</i>	6084	6834	7960	6578	6949	7729	8230
<i>harfbuzz</i>	9437	12178	10001	10025	9367	9829	9928
<i>objdump</i>	5177	6234	7377	5437	5326	5684	8363
<i>size</i>	2930	5528	4376	4245	2901	3075	5058
<i>nm</i>	3282	5566	5772	4817	3947	4630	6586
<i>strip</i>	4846	10086	8065	6473	5016	n/a	9457

n/a indicates that we are unable to instrument programs or failed to run the fuzzer

TABLE 2: Detailed edge coverage of different fuzzers

5.1 Edge coverage

To answer RQ1, we fuzz each program for 24 hours and 3 times. Then, we report the average results. Since each fuzzing process of Neuzz occupies an entire GPU (e.g., 10 GB) for 24 hours, we do not have sufficient GPU resources to run Neuzz multiple times. As a result, unlike other fuzzers, each program is fuzzed once with Neuzz. According to our experiment settings, Neuzz employs AFL for 1 hour to generate the initial training data, because of this, we only draw its last 23 hours. Note that this is also the same setting applied in their paper [9]. Although Angora and Finch uses the same method to measure edge coverage, the number of covered edges counted in Angora and Finch are different given the same set of test inputs. To avoid this incomparable edge coverage problem, we run Angora’s generated test inputs with Finch’s instrumented binaries to re-compute edge coverage. By applying this conversion, only edge coverage achieved by Angora after 24 hours is computed and thus, a single value is plotted. Similar to Angora, we also convert TortoiseFuzz’s edge coverage. The results are shown in Fig. 5 and the accumulated edge coverage after 24 hours are listed in Table 2.

From Fig. 5, we observe that on 6 out of 10 programs, Finch achieves the highest edge coverage. Especially, it outperforms other fuzzers with a large margin in programs *objdump* and *nm*. For the remaining programs, Finch is the second best fuzzer except *harfbuzz*. It is not surprise that Angora achieves relatively high edge coverage. Angora is benefited from a search algorithm based on gradient descent, which is similar to our hot-bytes mutation. Although Neuzz is guided by gradient-guided mutation, it is unable to defeat other AFL-liked fuzzers, i.e., MOPT and Fairfuzz. In two programs *djpeg* and *xmllint*, Neuzz is even the worst fuzzer. TortoiseFuzz achieves the lowest edge coverage in many programs (e.g., *libpng*, *tiffcp*, *nm*, *strip*) because its mutation strategy favors test inputs containing memory operations. Among 10 programs, *bzip2* has low stability (i.e., two runs with the same input may result in 2 different execution paths). Because of this, its edge coverage measurement could be inaccurate.

A closer investigation shows that, in most of the cases, Finch typically starts with a low edge coverage, gradually goes up and then surpasses MOPT at around 15 hours. This is an expected behaviour as Finch initially has limited guidance from the neural network and gradually builds

on program-specific knowledge to evolve the seed pool towards covering uncovered branches. This optimization process is time-consuming. We do believe that Finch will create even larger margin if the programs are fuzzed for a longer time. This is because we still see the upward trend of Finch when the 24-hour limit is reached.

According to our results, it is clear that the overall ranking of 7 fuzzers is Finch > Angora > MOPT > Fairfuzz > Neuzz > AFL > TortoiseFuzz. Compared to Neuzz which similarly uses neural networks to predict hotbytes, we achieve 1.2x more edge coverage across multiple target programs.

Program	Angora	Finch	MOpt
<i>djpeg</i>	2463 / 2478 / 6	2500 / 2607 / 49	2588 / 2621 / 14
<i>harfbuzz</i>	12008 / 12263 / 120	9897 / 9951 / 23	9856 / 10072 / 102
<i>libpng</i>	2947 / 2953 / 3	3013 / 3073 / 25	2955 / 2962 / 3
<i>nm</i>	5368 / 5790 / 173	6168 / 6837 / 298	5242 / 6094 / 377
<i>objdump</i>	5888 / 6662 / 321	8005 / 8655 / 270	7195 / 7543 / 142
<i>size</i>	5343 / 5629 / 131	4529 / 5341 / 375	4292 / 4535 / 113
<i>strip</i>	9309 / 10630 / 564	8865 / 10173 / 541	7857 / 8172 / 147
<i>tiffcp</i>	6791 / 6919 / 60	8097 / 8390 / 121	7923 / 8028 / 48

TABLE 3: Edge ranges of 3 top fuzzers across different runs

To provide greater detail on the result of multiple runs, we show the ranges and standard deviations of 3 top fuzzers in the Table 3 where each cell has the format (min / max / std). It can be seen that the results across multiple runs are relatively stable.

5.2 Branch distance bitmap

Program	Edge coverage bitmap	Branch distance bitmap
<i>djpeg</i>	2	7
<i>xmllint</i>	140	107
<i>libpng</i>	13	56
<i>tiffcp</i>	353	227
<i>harfbuzz</i>	33	46
<i>objdump</i>	298	237
<i>size</i>	102	112
<i>nm</i>	69	104
<i>strip</i>	135	147

TABLE 4: Detailed edge coverage

In Neuzz paper, a closely related work, its neural network is trained with edge coverage bitmap. Therefore, to answer RQ2, we compare edge coverage achieved from test inputs generated by two neural networks: (1) using branch distance bitmap and (2) using edge coverage bitmap. Both networks are trained with the same training data, which is the min-Pareto set of AFL’s seed pool achieved after 24 running hours. Then, the entire seed pool is mutated using Algorithm 3. The details on the achieved edge coverage are shown in Table 4.

From the table, we observe that branch distance bitmap has higher edge coverage than edge coverage bitmap in 6 out of 9 programs including *djpeg*, *libpng*, *harfbuzz*, *size*, *nm* and *strip*. We also notice that coverage bitmap is better than branch distance bitmap on programs containing many easy-to-cover branches which have not been covered. For example, it helps to cover 353 branches in *tiffcp* and 298

branches in *objdump*, these number of covered branches are significantly larger than in other programs, e.g., 2 in *djpeg* and 13 in *libpng*. We believe that when not so many easy-to-cover branches remain (e.g., programs are executed for a longer time), our proposed branch distance bitmap will dominate its opponent, edge coverage bitmap, in term of guiding the mutation process to discover new branches. This is evidenced by the experiment results on RQ1.

It can be observed that the branch distance bitmap works better in most of the programs as expected. For some programs, however, if the edge coverage bitmap is able to offer useful guidance (e.g., when the covered and uncovered branches share the same hot-bytes), it may still be effective. The worst case scenario for edge coverage bitmap occurs when there are a small number of new covered branches. In other words, easy-to-cover branches are mostly covered and the machine learning model offers little information on what are the hot-bytes for covering the remaining branches. The results from Fig. 5 partially confirms our analysis. For most of the programs, while edge coverage achieved by Neuzz becomes fixed after 5 hours, Finch maintains the upward trend throughout the whole process.

5.3 Min-Pareto set

To answer RQ3, we reuse the training data of the experiments in Section 5.2. The neural network is trained with branch distance bitmap. We measure the number of test inputs of a seed pool a.k.a pool size, edge coverage and number of executions in two settings: (1) mutating the min-Pareto set and (2) mutating AFL’s seed pool.

Fig. 6 shows the summarized results from the two settings where x-axis represents target programs and y-axis is the unit of measured metrics. From the figure, we observe that our pool size is always much smaller than AFL’s seed pool. On average, it accounts for 11.72% of AFL’s seed pool. Since a smaller pool results in a smaller number of generated test inputs and thus less executions, on average, our strategy executes 11.11% test inputs but achieves 87.48% edge coverage in comparison with AFL’s seed pool. In some rare cases (e.g., *libpng*), with less test inputs, the min-Pareto set allows us discover more edges than mutating entire AFL’s seed pool. This suggests that training neural network models with as many test inputs as possible is not always a good idea. This is because the training data is likely imbalanced, i.e., some paths are executed more often than others given the AFL’s seed pool.

5.4 Detecting bugs

Artificial Dataset. LAVA-M has a set of synthetic bugs inserted to 4 real-world programs *base64*, *md5sum*, *uniq*, *who* from project *coreutils-8.24*. It is commonly used to measure the ability of discovering bugs of modern fuzzers [4], [5], [22]. In LAVA-M, a bug is identified by a unique number and guarded by a 4-byte comparison as shown in Figure 7 (lines 2-3) where a bug is counted if the true-branch (lines 2-3) is satisfied. Considering a simple expression *lava_get(0) + lava_get(1) + lava_get(2)* leading to bugs 0, 1 and 2. Due to the deduplication mechanism of Finch, whenever a bug is discovered (e.g., bug 0), remaining bugs (e.g., 1 and 2) will be discarded and not counted in our final results, even

	base64	md5sum	uniq	who
# Bugs	44	57	28	2136
Fuzzer	7	2	7	0
SES	9	0	0	18
VUZZER	17	1	27	50
Steelix*	43	28	7	194
Angora	48	57	29	1541
T-Fuzz	43	49	26	63
RedQueen	44	57	28	2134
GREYONE*	44	57	28	2136
Matryoshka*	48	57	29	2432
Neuzz	48	60	29	1582
Finch	48	61	29	2229

* indicates that the fuzzer is not opensource

TABLE 5: Number of bugs found by different fuzzers on LAVA-M dataset

if they are triggered. This is because the remaining bugs do not achieve new coverage as bug 0 already bypassed the true-branch at line 2-3. To avoid such problem, we transform the above expression to $hf0(0) + hf1(1) + hf2(2)$ where functions *hf0*, *hf1*, *hf2* are identical to *lava_get*. In the transformed version, the behavior of the original program is unchanged. However, each bug is associated with a unique branch and thus, the number of bugs is accurately counted in our final results. We apply this transformation to LAVA-M, conduct experiments and report the number of bugs found by Finch in Table 5. We compare our results with 7 other fuzzers where their number of bugs are taken from corresponding papers [1], [4], [5], [8], [9], [22], [23].

Finch found the highest in number of bugs in 3 out of 4 programs. Especially, only Finch is able to discover 61 bugs in program *md5sum*. Additionally, it triggers many unlisted bugs in LAVA-M. Finch takes less than 1 hour to discover 48 and 29 bugs in *md5sum* and *uniq* respectively. After 6 hours, 61 bugs of *md5sum* are exposed. For the slowest program *who*, 2229 bugs are found within 24 hours. The outstanding results confirm that Finch accurately selects the hot-bytes, mutate them to bypass magic-bytes comparisons.

Real-world Applications. Besides traditional crashes, to detect memory related bugs that does not necessarily cause a crash, we compile 10 real-world programs with ASAN. We run the same 6 fuzzers for 24 hours and report unique bugs found in Table 6. Note that the results are obtained after removing false positive and duplicated crashes. From Table 6, we observe that Finch and Angora discover 1 previously unknown bug in program *tiffcp* and *strip* respectively, whereas all other fuzzers discover nothing.

Program	Tortoise Fuzz	Angora	MOPT	FairFuzz	AFL	Neuzz	Finch
<i>tiffcp</i>	0	0	0	0	0	0	1
<i>strip</i>	0	1	0	0	0	0	0
<i>others</i>	0	0	0	0	0	0	0

TABLE 6: Unique bugs found by different fuzzers

5.5 Training overhead

To support hot-bytes mutation, Finch introduces extra training time compared to AFL. Therefore, to answer RQ5, we measure the amount of time that the training task takes

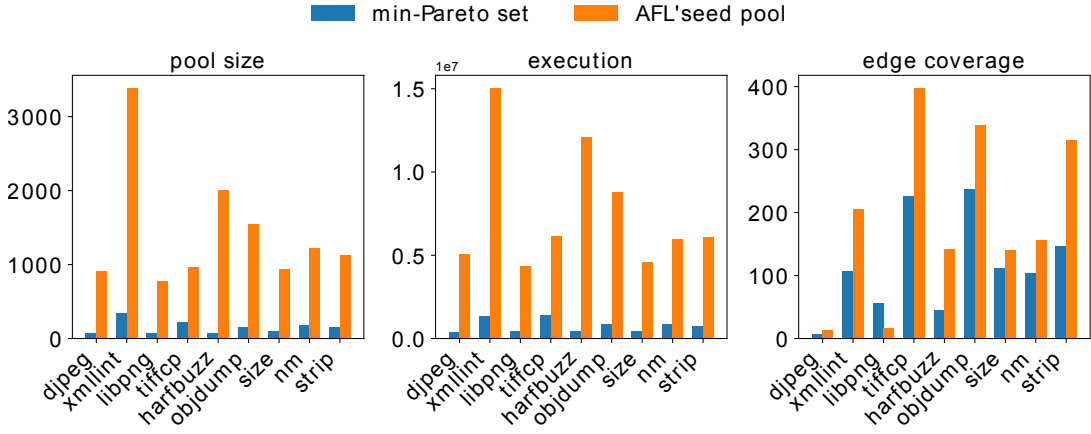


Fig. 6: AFL's seed pool versus min-Pareto set

```

1 unsigned int lava_get(unsigned int bug_num) {
2   if (0x6c617661 - bug_num == lava_val[bug_num]
3     || SWAP_UINT32(0x6c617661 - bug_num) ==
4       lava_val[bug_num]) {
5     printf("Successfully triggered bug %d,
6       crashing now!\n", bug_num);
7   }
8   return lava_val[bug_num];
9 }

```

Fig. 7: A bug is triggered at function lava_get()

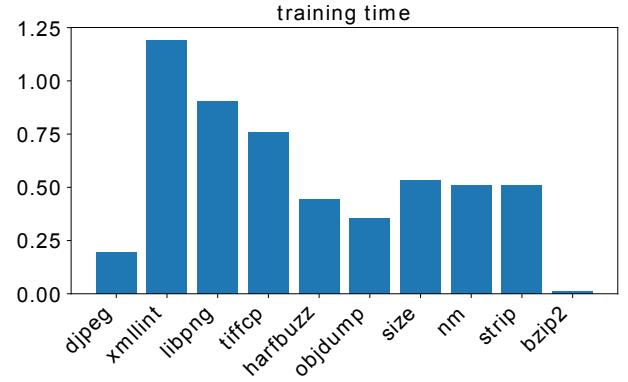


Fig. 8: Training time of Finch running for 24-hour experiments

during our 24-hour experiments. Fig. 8 summarizes the experiment results collected from 10 programs where y-axis is accumulated time in hours from multiple trainings during the lifetime of Finch. From Fig. 8 we observe that in program *xmllint*, Finch spends around 1.19 hours to train multiple min-Pareto sets. This is because *xmllint* is a complicated program which has many uncovered branches recorded as the training labels, e.g., the number of just-missed branches are 3449 when Finch runs for 24 hours. In contrast, program *bzip2* is relatively small and thus the training time is insignificant. Intuitively, programs with many branches may result in more training time. On average, Finch spends 0.54 hours for training. This amount of time is a reasonable trade-off to achieve better mutation results.

6 RELATED WORK

Finch is closely related to machine learning based-fuzzers. Mohit Rajpal et al. [24] employs multiple neural network architectures (e.g., LSTMs and sequence-to-sequence) to learn patterns in test inputs and guide the process of AFL's test input generation to reduce the number of useless mutations. Neuzz [9] uses gradient scores learned from a trained feed-forward neural network which approximates program's branching behaviours to assist the process of mutating hot-bytes (gradient-guided mutation). In [9], She et al. presented MTFuzz which is built on top of Neuzz. MTFuzz combines multiple training labels (i.e., edge-coverage, approach-sensitive and context-sensitive) to improve the accuracy of hot-bytes prediction. However, MTFuzz similarly suffers

from the limitations of Neuzz. Machine learning techniques were also applied to different fuzzing steps, e.g., seed pool selection [25], [26] and test input mutation [27], [28].

Finch is complementary to existing fuzzers relying on search-based software testing approach. MooFuzz [29] formulates test input selection and energy allocation as a many-objective optimization problem. Their mutated test inputs increase path risk and decrease energy consumption. sFuzz [13] is a smart contract fuzzer which employs a lightweight multi-objective adaptive strategy targeting those hard-to-cover branches to achieve new coverage. Essentially, it spends more effort on mutating a test input that is the best for a just-missed branch.

Finch is related to fuzzers that analyze data flow dependency to identify promising mutating locations. Matryoshka [22] collects predicates in the conditional statement that guards uncovered branches and analyzes related control and data flow dependency to generate test inputs that can easily bypass constraints involving deeply nested conditional statements. Angora [5] uses byte-level taint tracking to determine hot-bytes and bypass complicated constraints by mutating test inputs with the guidance of gradient descent algorithm. GREYONE [4] infers taint of variables and uses this information to prioritize uncovered branches, bytes in the mutation algorithms. The data dependency analysis

were also applied in many other fuzzers, e.g., REDQUEEN [8], Vuzzer [2], Steelix [1] and TaintScope [30]. Compared with the above-mentioned approaches, Finch quantifies the dependency with the help of a neural network trained with branch distances.

Finch is broadly related to fuzzers that uses symbolic/concolic execution techniques to solve path constraints. SAVIOR [7] prioritizes the concolic execution of the seed that are likely to discover more vulnerabilities. Driller [6] uses its fuzzing engine to explore most of the execution paths and switch to concolic execution only to bypass complicated conditions. T-fuzz [23] fuzzes transformed programs to get out of stuck and leverages crash analyzers to remove false positives. Unfortunately, this approach often suffer from reliability and performance issues in practice.

7 CONCLUSION

In this work, we propose an approach to solve 2 fundamental problems in fuzzers, i.e., how to choose the seed and which bytes to mutate so that we can maximize the coverage as well as discover more bugs. Our approach is based on the idea that we can use the distances between test inputs and uncovered branches to choose the test inputs to mutate and to train a neuron network model which can help to guide the mutation process. The experiment results on popular programs show that our approach outperforms state-of-the-art tools. Currently, our implementation is for C/C++ programs. In future, we plan to extend our approach into a framework which can support the fuzzing of programs written in different languages.

REFERENCES

- [1] Y. Li, B. Chen, M. Chandramohan, S.-W. Lin, Y. Liu, and A. Tiu, "Steelix: program-state based binary fuzzing," in *Proceedings of the 2017 11th Joint Meeting on Foundations of Software Engineering*, 2017, pp. 627–637.
- [2] S. Rawat, V. Jain, A. Kumar, L. Cojocar, C. Giuffrida, and H. Bos, "Vuzzer: Application-aware evolutionary fuzzing," in *NDSS*, vol. 17, 2017, pp. 1–14.
- [3] D. She, R. Krishna, L. Yan, S. Jana, and B. Ray, "Mtfuzz: Fuzzing with a multi-task neural network," *arXiv preprint arXiv:2005.12392*, 2020.
- [4] S. Gan, C. Zhang, P. Chen, B. Zhao, X. Qin, D. Wu, and Z. Chen, "Greyone: Data flow sensitive fuzzing," in *29th USENIX Security Symposium (USENIX Security 20)*. USENIX Association, Boston, MA, <https://www.usenix.org/conference/usenixsecurity20/presentation/gan>, 2020.
- [5] P. Chen and H. Chen, "Angora: Efficient fuzzing by principled search," in *2018 IEEE Symposium on Security and Privacy (SP)*. IEEE, 2018, pp. 711–725.
- [6] N. Stephens, J. Grosen, C. Salls, A. Dutcher, R. Wang, J. Corbetta, Y. Shoshitaishvili, C. Kruegel, and G. Vigna, "Driller: Augmenting fuzzing through selective symbolic execution," in *NDSS*, vol. 16, no. 2016, 2016, pp. 1–16.
- [7] Y. Chen, P. Li, J. Xu, S. Guo, R. Zhou, Y. Zhang, T. Wei, and L. Lu, "Savior: Towards bug-driven hybrid testing," in *2020 IEEE Symposium on Security and Privacy (SP)*. IEEE, 2020, pp. 1580–1596.
- [8] C. Aschermann, S. Schumilo, T. Blazytko, R. Gawlik, and T. Holz, "Redqueen: Fuzzing with input-to-state correspondence," in *NDSS*, vol. 19, 2019, pp. 1–15.
- [9] D. She, K. Pei, D. Epstein, J. Yang, B. Ray, and S. Jana, "Neuzz: Efficient fuzzing with neural program smoothing," in *2019 IEEE Symposium on Security and Privacy (SP)*. IEEE, 2019, pp. 803–817.
- [10] A. Panichella, F. M. Kifetew, and P. Tonella, "Automated test case generation as a many-objective optimisation problem with dynamic selection of the targets," *IEEE Transactions on Software Engineering*, vol. 44, no. 2, pp. 122–158, 2017.
- [11] P. McMinn, "Search-based software test data generation: a survey," *Software testing, Verification and reliability*, vol. 14, no. 2, pp. 105–156, 2004.
- [12] M. Harman and P. McMinn, "A theoretical and empirical study of search-based testing: Local, global, and hybrid search," *IEEE Transactions on Software Engineering*, vol. 36, no. 2, pp. 226–247, 2009.
- [13] T. D. Nguyen, L. H. Pham, J. Sun, Y. Lin, and Q. T. Minh, "sfuzz: An efficient adaptive fuzzer for solidity smart contracts," *arXiv preprint arXiv:2004.08563*, 2020.
- [14] M. Zalewski. american fuzzy lop. [Online]. Available: <https://github.com/google/AFL>
- [15] C. Lemieux and K. Sen, "Fairfuzz: A targeted mutation strategy for increasing greybox fuzz testing coverage," in *Proceedings of the 33rd ACM/IEEE International Conference on Automated Software Engineering*, 2018, pp. 475–485.
- [16] C. Lyu, S. Ji, C. Zhang, Y. Li, W.-H. Lee, Y. Song, and R. Beyah, "Mopt: Optimized mutation scheduling for fuzzers," in *28th USENIX Security Symposium (USENIX Security 19)*, 2019, pp. 1949–1966.
- [17] Y. Wang, X. Jia, Y. Liu, K. Zeng, T. Bao, D. Wu, and P. Su, "Not all coverage measurements are equal: Fuzzing by coverage accounting for input prioritization," in *NDSS*, 2020.
- [18] R. Padhye, C. Lemieux, K. Sen, L. Simon, and H. Vijayakumar, "Fuzzfactory: domain-specific fuzzing with waypoints," *Proceedings of the ACM on Programming Languages*, vol. 3, no. OOPSLA, pp. 1–29, 2019.
- [19] LLVM, "LibFuzzer," <https://llvm.org/docs/LibFuzzer.html>, 2022, [Online; accessed 27-Feb-2022].
- [20] T. Yue, P. Wang, Y. Tang, E. Wang, B. Yu, K. Lu, and X. Zhou, "Ecofuzz: Adaptive energy-saving greybox fuzzing as a variant of the adversarial multi-armed bandit," in *29th {USENIX} Security Symposium ({USENIX} Security 20)*, 2020, pp. 2307–2324.
- [21] Google, "FuzzBench," <https://www.fuzzbench.com>, 2020, [Online; accessed 07-May-2021].
- [22] P. Chen, J. Liu, and H. Chen, "Matryoshka: fuzzing deeply nested branches," in *Proceedings of the 2019 ACM SIGSAC Conference on Computer and Communications Security*, 2019, pp. 499–513.
- [23] H. Peng, Y. Shoshitaishvili, and M. Payer, "T-fuzz: fuzzing by program transformation," in *2018 IEEE Symposium on Security and Privacy (SP)*. IEEE, 2018, pp. 697–710.
- [24] M. Rajpal, W. Blum, and R. Singh, "Not all bytes are equal: Neural byte sieve for fuzzing," *arXiv preprint arXiv:1711.04596*, 2017.
- [25] J. Wang, B. Chen, L. Wei, and Y. Liu, "Skyfire: Data-driven seed generation for fuzzing," in *2017 IEEE Symposium on Security and Privacy (SP)*. IEEE, 2017, pp. 579–594.
- [26] Y. Wang, Z. Wu, Q. Wei, and Q. Wang, "Neufuzz: Efficient fuzzing with deep neural network," *IEEE Access*, vol. 7, pp. 36 340–36 352, 2019.
- [27] Y. Li, S. Ji, C. Lyu, Y. Chen, J. Chen, Q. Gu, C. Wu, and R. Beyah, "V-fuzz: Vulnerability prediction-assisted evolutionary fuzzing for binary programs," *IEEE Transactions on Cybernetics*, 2020.
- [28] K. Böttinger and C. Eckert, "Deepfuzz: Triggering vulnerabilities deeply hidden in binaries," in *International Conference on Detection of Intrusions and Malware, and Vulnerability Assessment*. Springer, 2016, pp. 25–34.
- [29] X. Zhao, H. Qu, W. Lv, S. Li, and J. Xu, "Moofuzz: Many-objective optimization seed schedule for fuzzer," *Mathematics*, vol. 9, no. 3, 2021. [Online]. Available: <https://www.mdpi.com/2227-7390/9/3/205>
- [30] T. Wang, T. Wei, G. Gu, and W. Zou, "Taintscope: A checksum-aware directed fuzzing tool for automatic software vulnerability detection," in *2010 IEEE Symposium on Security and Privacy*. IEEE, 2010, pp. 497–512.